International Journal of Sustainable Development and Planning
Vol. 20, No. 12, December, 2025, pp. 5313-5325
Journal homepage: http://iieta.org/journals/ijsdp

Integration of Theoretical and Practical Parameters for the Geotechnical Characterization of a Small-Scale Landslide, Zaruma-Ecuador

Joselyne Solórzano[1,2*], Samuel Haro[3], Jean Espinoza-Chamba[3], Miguel Torres-Campozano[3], Jennifer Cueva-Medina[1], Emily Sánchez-Zambrano[1,2], Paúl Carrión-Mero[1,2], Fernando Morante-Carballo[1,4,5]

[1] Centro de Investigación y Proyectos Aplicados a las Ciencias de la Tierra (CIPAT), ESPOL Polytechnic University, ESPOL, Campus Gustavo Galindo, Guayaquil 090902, Ecuador
[2] Facultad de Ingeniería en Ciencias de la Tierra (FICT), ESPOL Polytechnic University, ESPOL, Campus Gustavo Galindo, Guayaquil 090902, Ecuador
[3] Facultad de Ciencias Naturales, Universidad de Guayaquil, Guayaquil 090613, Ecuador
[4] Facultad de Ciencias Naturales y Matemáticas (FCNM), ESPOL Polytechnic University, ESPOL, Campus Gustavo Galindo, Guayaquil 090902, Ecuador
[5] Geo-Recursos y Aplicaciones (GIGA), ESPOL Polytechnic University, ESPOL, Campus Gustavo Galindo, Guayaquil 090902, Ecuador

Corresponding Author Email: josbasol@espol.edu.ec

Copyright: ©2025 The authors. This article is published by IIETA and is licensed under the CC BY 4.0 license (http://creativecommons.org/licenses/by/4.0/).

https://doi.org/10.18280/ijsdp.201223

Received: 7 November 2025
Revised: 6 December 2025
Accepted: 26 December 2025
Available online: 31 December 2025

Keywords:
mitigation strategies, Safety Factors, geophysical, geotechnical, mass movement, colluvial soil, SWOT, rural planning

ABSTRACT

Landslides are among the most recurrent natural hazards in Ecuador, triggered by a combination of geological, geomorphological, and anthropogenic factors. In the Sinsao parish of Zaruma city, a large-scale landslide has persisted for over a decade, affecting infrastructure and posing a threat to residents. This study analyzes a small-scale landslide within the same process, which shows signs of reactivation despite previous interventions. Given limited accessibility and economic constraints that restrict conventional geotechnical studies, an alternative methodological approach integrates theoretical geotechnical parameters with geospatial and geotechnical modelling software to estimate the Safety Factor (SF) and propose potential mitigation strategies. The research followed three phases: (i) collection of geophysical, geotechnical, and bibliographic data; (ii) data integration and modeling the SF; and (iii) participatory action plan. Results indicated that, on the slope composed predominantly of coarse sandy clay, 25% of the area has a SF below 1.5 according to the geospatial software zoning the most affected areas, and geotechnical modeling showed values of 0.99 (static) and 0.56 (pseudo-static) on the most significant terrain slope, both below the threshold of the Ecuadorian Construction Standard (NEC), highlighting the need for immediate preventive measures. This methodological approach demonstrates the feasibility of conducting reliable preliminary assessments in remote areas, supporting risk management, territorial planning, and urgent mitigation in vulnerable communities.

1. INTRODUCTION

Mass movements are common geodynamic processes in mountainous areas and continuously threaten populations and infrastructure [1]. The standard classification of mass movements is based on the type of movement and the material that slides. Five groups are identified: falls, toppling, flows, extensions, and landslides [2]. The main factors that trigger landslides are classified based on temporal scale into short-term (e.g., earthquakes, rainfall, volcanic activity), medium-term (e.g., tectonic activity, depositional loading), and long-term (e.g., sea-level changes). These events are studied using both direct and indirect methods, enabling the development of effective mitigation strategies for landslide characterization.

Direct methods include laboratory tests and in-situ techniques that provide accurate data but often involve access difficulties and high costs. Indirect methods use secondary data sources, such as geophysical data. Standard geophysical methods in landslide characterization include Electrical Resistivity Tomography (ERT), Vertical Electrical Sounding (VES), and seismic refraction (SR). Tools such as remote sensing, Geographic Information Systems (GIS), and artificial intelligence (AI) are also implemented [3].

Recent studies show that combining geophysical methods with shallow geotechnical testing effectively identifies water-saturated zones, structural discontinuities, and lithological variations linked to instability [4]. Laboratory tests provide accuracy but often involve logistical challenges that are impractical in unstable or remote areas [5]. Geophysical techniques such as ERT and RS can produce high-resolution profiles but are expensive, sensitive to noise, and require specialized personnel [6]. GIS and AI tools, although flexible

and cost-effective, depend heavily on data quality and the robustness of training datasets [7]. These limitations emphasize the importance of developing methods tailored to local conditions to ensure dependable, reproducible results in complex environments. Case studies from regions such as the Northern Apennines [3], the Himalayas [8], and Brazil [9] highlight the successful integration of geotechnical and geophysical methods in landslide analysis. Both open-source software, such as the System for Automated Geoscience Analysis (SAGA GIS), and commercial platforms, such as Slide2, enable the inclusion of topographic, geotechnical, and geophysical data in slope stability models.

In Ecuador, significant rainfall, steep slopes, unconsolidated soils, and vibrations from seismic or mining activities are primary triggers of landslides [10]. These natural factors are further exacerbated by socioeconomic challenges, such as unregulated urban development and the absence of geotechnical regulations for civil works [11]. Historically, Ecuador has repeatedly experienced catastrophic landslides, such as those in Chunchi (1983), La Josefina (1993), and Alausí (2023), which have resulted in hundreds of fatalities [12]. In this sense, the development of efficient methodologies for slope characterization and stability analysis is essential to fostering resilient communities [13].

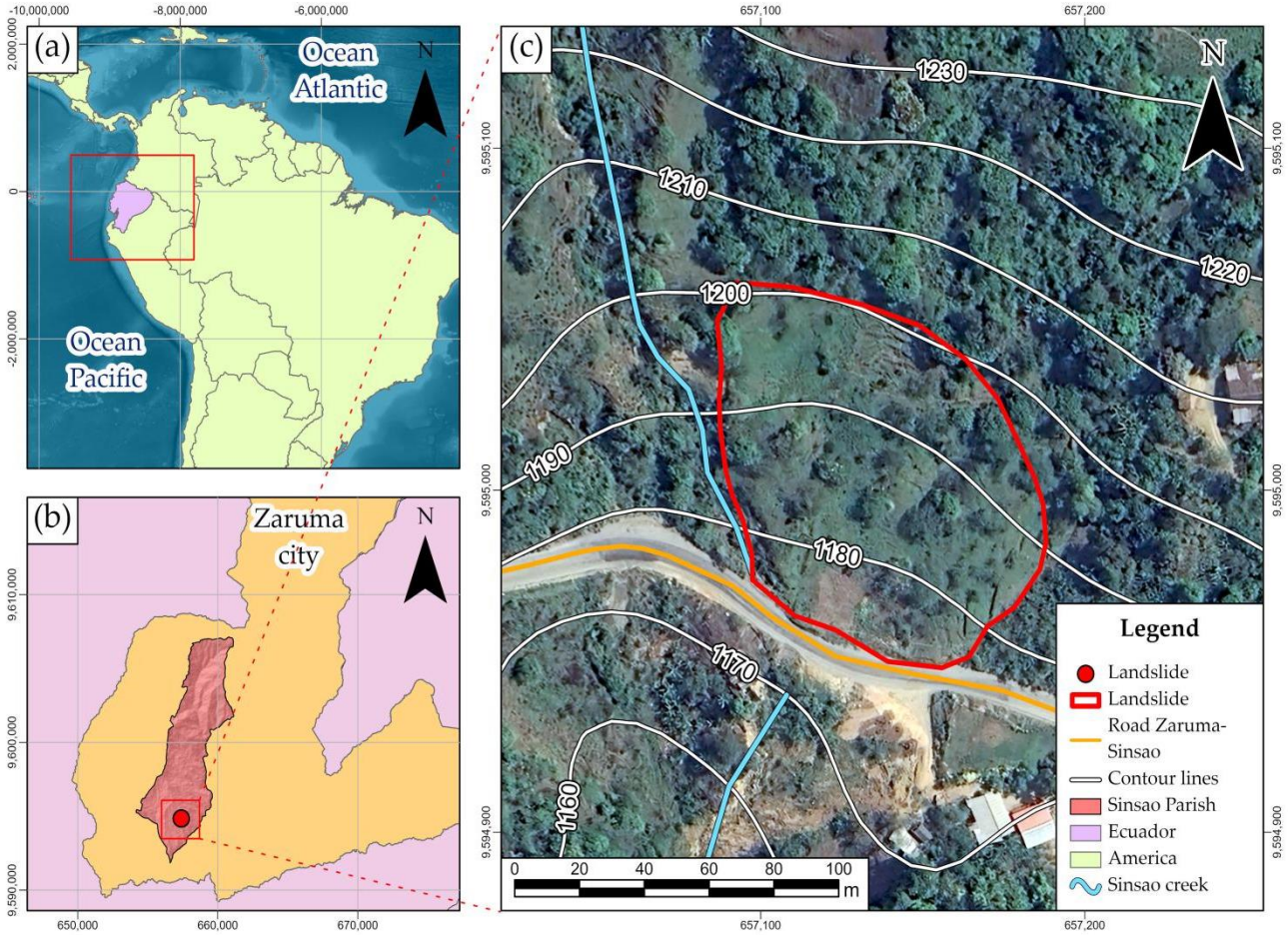

Figure 1. The location map of the study area limited the Sinsao Creek. a) Ecuador; b) Zaruma; c) Small-scale landslide

The Sinsao parish in the Zaruma city faces critical landslide conditions due to its irregular topography, informal mining activity, insufficient geological studies, and high rainfall [14]. This area is affected by a large-scale landslide complex that has been active for more than a decade, causing significant damage to infrastructure and posing a persistent threat to the local population (Figure 1). The study area, located north of the Zaruma-Sinsao highway, exhibits steep escarpments, surface cracks, and areas of water accumulation, leading to progressive slope deformation. Given the emergency context and the need to assess slope stability under limited logistical and economic conditions, this research focuses on developing a methodological approach for stability assessment in remote environments with limited resources. The following question arises: How can integrate theoretical and practical data on an open-source GIS platform, such as SAGA GIS, with geotechnical software, such as Slide2, to produce slope stability estimates for landslide analysis in remote locations? This study explores a methodological alternative for landslide characterization by combining theoretical geotechnical parameters with specialized software, such as SAGA GIS and Slide2, to develop mitigation strategies that enable land-use planning in disadvantaged areas.

2. MATERIALS AND METHODS

2.1 Geographical and demographic context

This study is focused on Ecuador (Figure 1 (a)), specifically on a landslide located along the roadside in Sinsao parish (795851590 W-36629693 S) (Figure 1 (b)), situated in the foothills of the Andes Mountains at an elevation of 1,280 m above sea level (m.a.s.l.). The area has a humid forest climate,

with an average annual precipitation of 1,900-2,000 mm [15] (Figure 1 (c)). According to the 2022 national census, the parish has a population of 1,594 inhabitants, with mining being the primary economic activity (40.83%), followed by agriculture, livestock, forestry, and fishing (12%) [16]. According to the latest Parish Land Use and Development Plan (PDOT, Spanish acronym), the study area experiences recurrent landslides during the rainy season [15]. In 2015, the National Risk Management Secretariat (SNGR, Spanish acronym) mapped 25 landslides along the Sinsao road after a single night of intense rainfall [17]. Additionally, in 2018, the area was officially designated as a high-risk landslide zone [10].

2.2 Geologic context

Sinsao parish is located within a geologically complex region characterized by high fracturing, altered volcano-sedimentary lithologies, and active tectonics. The area is part of the Zaruma-Portovelo metallogenic belt, which consists mainly of intrusive rocks, andesites, dacites, and colluvial-alluvial deposits [18].

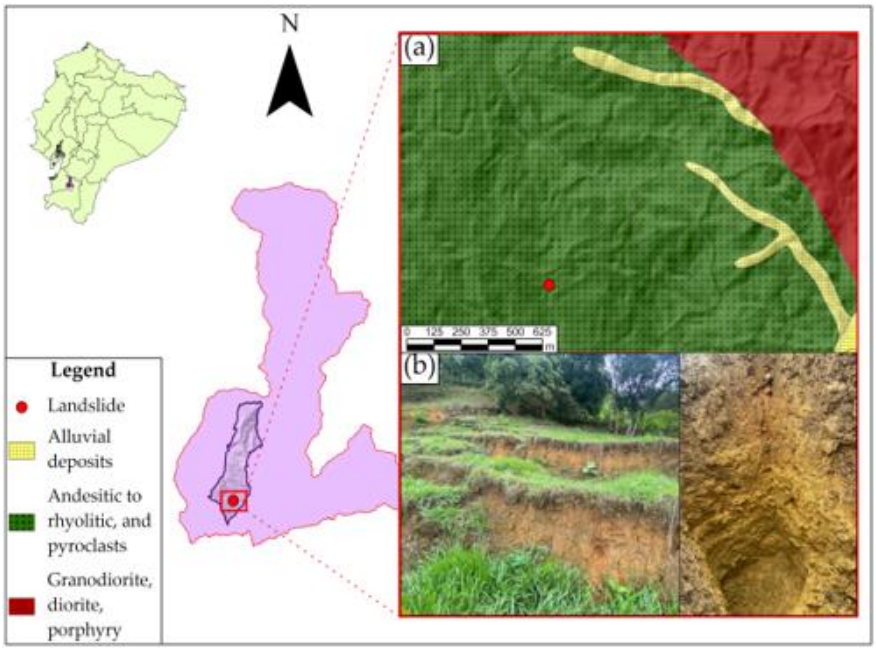

Figure 2. Geologic map: a) Lithological features, b) Exposed soil observed in escarpments and through pits test

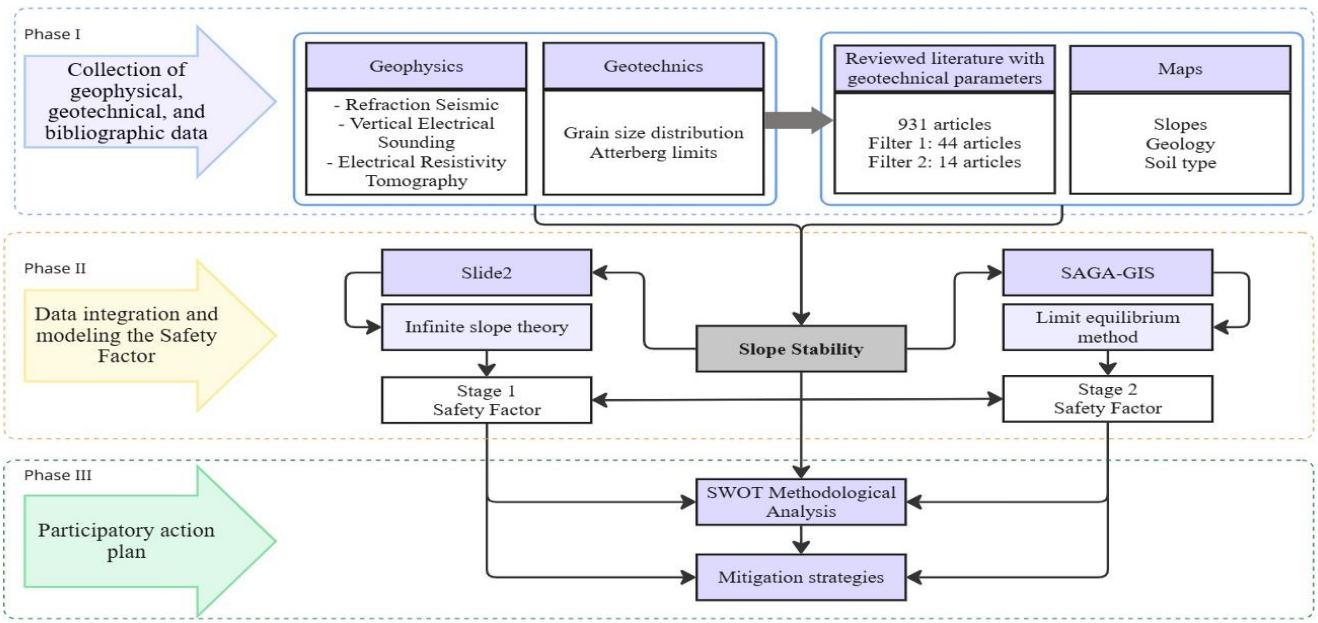

Figure 3. Schematic representation of the research approach and phases in slope stability analysis

The geology in the study area belongs to the Saraguro group, consisting of calc-alkaline volcanic rocks of Oligocene age, the Portovelo unit (Figure 2(a)), bounded by the Piñas-Portovelo fault [19]. Upon weathering, this material has formed clayey, sandy, and sandy clayey soils, known as saprolites, with thicknesses ranging from 20 to 30 m, highly unstable (Figure 2(b)) [14, 20].

2.3 Methodological framework

This study integrated geotechnical evaluation techniques, including granulometry tests and Atterberg limits, with geophysical methods such as ERT, RS, and VES. The investigation was structured in three methodological phases (Figure 3). The first comprised ground reconnaissance and the collection of geotechnical and geophysical data through in situ tests and indirect techniques, complemented by the collection of geomechanical parameters and geological background collected in the scientific literature. The physical-mechanical and slope data were integrated and processed in SAGA GIS and Slide2 to estimate slope SF under different scenarios. Finally, a Strengths, Weaknesses, Opportunities, and Threats (SWOT) analysis was carried out to identify key factors, followed by a mitigation strategies approach aligned with the identified level of stability.

2.3.1 Phase I: Collection of geophysical, geotechnical, and bibliographic data

The recognition and delimitation of the landslide was carried out after a field visit, which verified the presence of escarpments at the top of the slope, moisture, cracks, and soil erosion at the base of the landslide (Figure 4).

Geomechanical considerations. Soil characterization was carried out using granulometry and Atterberg limit tests [21] at the ESPOL Geotechnical Laboratory, and the samples were classified according to the Unified Soil Classification System (USCS) [22]. Samples were taken from two test pits (1.20×1.55 m): the first at 0.70 m, 1.00 m, and 1.55 m depth; and the second at 0.70 m (Figure 4).

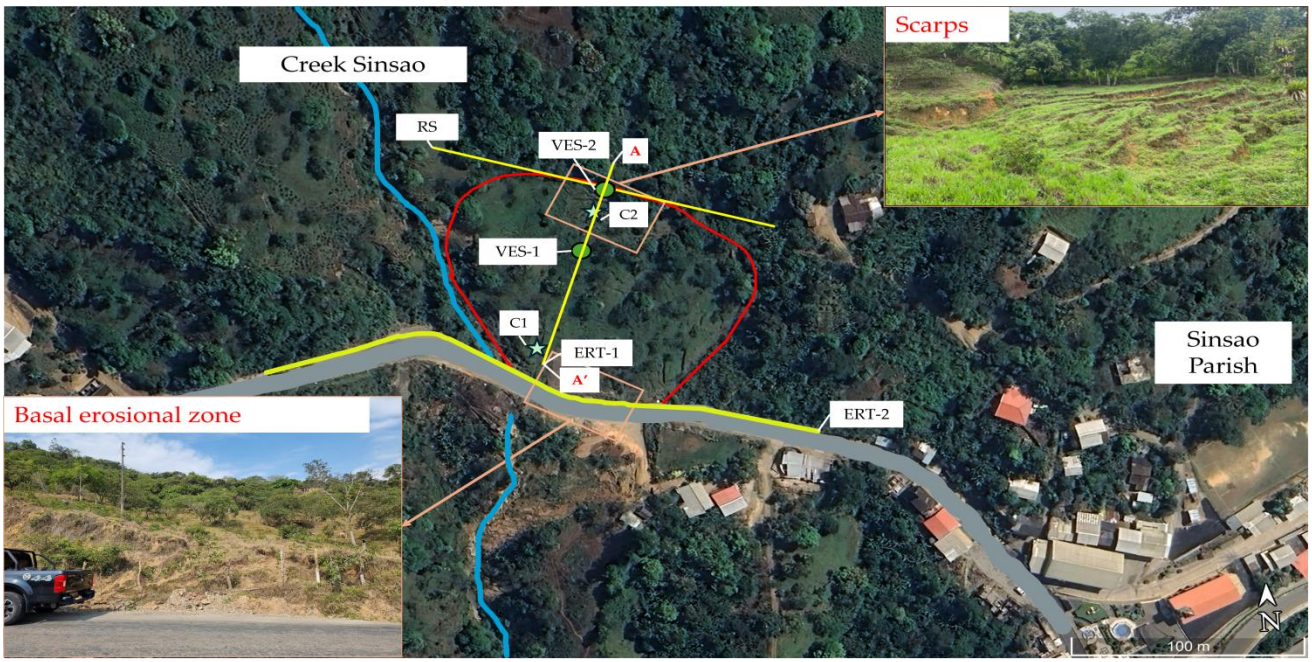

Figure 4. The map indicates the extent of a landslide, along with the locations of geophysical tests (ERT, VES, RS), test pits (C), and A-A' profile conducted within the affected area

Table 1. Keywords that make up the search equation in Scopus

Topics	Keywords
Mass movement	"landslide*" OR "slope failure*" OR "mass movement*"
Tests	"laboratory test*" OR "triaxial test*" OR "direct shear test*" OR "consolidation test*" OR "geotechnical characterization" OR "soil mechanics test*"
Parameters	"shear strength" OR "cohesion" OR "soil cohesion" OR "friction angle" OR "angle of internal friction" OR "soil density" OR "bulk density" OR "dry density" OR "soil saturation" OR "degree of saturation"

Geomechanical parameters used to calculate SF were obtained through a systematic search of the Scopus database of mass-movement studies. Three keywords were used: mass movement, laboratory tests, and geomechanical parameters and their synonyms, combined with the Boolean operator "OR". The three variables were then combined with the Boolean operator "AND" to extract documents containing only the three keywords. The search was further limited to papers published in Q1 journals and geotechnical values obtained solely from laboratory tests. Only documents in English published between 2019 and 2024 were considered (Table 1). Each article was evaluated based on soil type according to the USCS classification and geotechnical conditions like those of the study area to ensure data reliability (clayey soil). Finally, 13 articles were selected from which values of cohesion (c), internal friction angle (ϕ), density (ρ), saturation (s), and unit weight (γ) were extracted for use in slope stability modeling (see Table S1 in Appendix).

Geoelectric and seismic refraction measures. To characterize the subsurface and identify potentially unstable zones, five field tests were performed (Figure 4). Two ERT profiles were obtained using the ABEM Terrameter LS 2 with a gradient field array [23], comprising 41 electrodes arranged in 200 m lines, reaching depths of investigation of 20-40 m.

The resistivity data were processed with Res2dinv (v4.10.20), using the Root Mean Square (RMS) method to refine the model, eliminate noisy measurements, and generate four high-quality interpolations, which were essential for the subsequent delimitation of the stratigraphy.

The RS method included a 140 m profile with 24 geophones recording seismic velocities. The data were processed using

Reflexw software version 10.0, resulting in seismic tomography, where data quality was ensured by manually removing first-arrival noise on each strike. Two VES were measured using the Schlumberger configuration [24], with the Terrameter LS 2, with exploration lengths of up to 380 m and depths of investigation close to 70 m. The data were interpreted with IPI2win (v.3.0.1) to determine resistivities and thicknesses of subsurface layers comparing with the resistivities and thicknesses found in the ERT (Table 2).

Table 2. Resistivity and velocity ranges adapted to the case study

Material	Resistivity (Ω·m)	Velocity (m/s)	Autor
Very saturated saprolite	0-30		[25
Saturated saprolite	30-60	>600	[25, 26]
Slightly saturated saprolite / Soft soil with coarse	60-300	500-25	[27, 28]
Fractured saprolite	>600		[28]

Table 3. Input configuration for calculating the Safety Factor (SF) in SAGA and Slide2

Imputs	SAGA GIS	Slide2
Slope grid	DEM 3×3 (rad)	
Thickness	ERT and VES (m)	ERT and VES (m)
Saturation	Dimensionless 0-1	
Friction	Bibliography (degree)	Bibliography (degree)
Density	Bibliography (g/cm³)	
Cohesion	Bibliography (MPa)	Bibliography (MPa)
Unit weight		Bibliography (KN/m³)
Water table	Test pits (m)	Test pits (m)

2.3.2 Phase II: Data integration and modeling the SF

SAGA GIS application for landslide zoning. To estimate the SF, SAGA GIS was used with the SafetyFactor tool, based on the infinite slope theory [29]. This model assumes that the fault plane is parallel to the ground surface and extends indefinitely, evaluating ground stability by calculating the ratio of resistive to sliding forces in each cell [30]. Using input data such as a slope raster, geomechanical soil properties from phase I (c, ϕ, ρ, s), and the depth of the fault plane determined through geophysical surveys within the study area, a continuous SF raster was produced. This raster was divided into five classes, which were then compared with the Ecuadorian Construction Standard (NEC, Spanish acronym) [31] to assess their stability. According to the NEC, a slope is considered stable if it has an SF of 1.5 under static conditions and normal groundwater levels, while under pseudo-static conditions, incorporating a seismic coefficient, the minimum acceptable SF is 1.05.

Slide2 application for stability analysis. Rocscience's Slide2 software was used for slope stability analysis, which estimates SF and the critical slip surface using limit equilibrium methods [32]. Using the topographic profile of the steepest slope surveyed in the field, geophysical data were incorporated to define the slope's stratigraphy and assign geotechnical properties (c, ϕ, γ) to each layer. The input data for each software used is detailed in Table 3.

The location of the water table was determined based on direct observations in test pits and interpreted geophysical data. With this information, two scenarios were developed: one under static conditions and another under pseudo-static conditions, incorporating the seismic design coefficients for the Zaruma area (horizontal coefficient (Zh): 0.30; vertical coefficient (Zv): 0.15) [33]. In both cases, the SF was calculated using the Bishop method [34], which involves dividing the slope into vertical slices and analyzing the force balance within each slice to determine the SF from the ratio of resistive to sliding forces along a circular failure surface, typical in clay soils or residual material [35].

2.3.3 Phase III: Participatory action plan

SWOT analysis is a common tool for assessing and identifying key factors in policy development and planning [36]. As the final phase of the study, a SWOT matrix was used to thoroughly evaluate the technical findings and their impact on the community. Based on criteria from geophysical, geotechnical, and geological experts, as well as the local and historical knowledge of community and political leaders—including the mayor, council members, and parish head—threats and weaknesses related to the landslide and population were identified.

This analysis helped recognize and leverage community strengths, transforming them into opportunities. Based on this strategic assessment, mitigation proposals were developed, tailored to the local context, to reduce vulnerability, guided by criteria of geotechnical stability, technical feasibility, and social acceptability. The focus was on prioritizing low-impact interventions that offer high community benefits.

3. RESULTS

3.1 Geotechnical-geophysical characterization of small-scape landslide

3.1.1 Physical-mechanical soil characterization

Table 4 presents the geotechnical properties of the soil within the designated landslide-prone zone, indicating the presence of coarse sandy clay. Notably, water accumulation was observed at a depth of 0.75 m during the excavation of test pits. The physical-mechanical parameters of the soil (c, ϕ, γ, ρ, s) were established based on recent studies on soils similar to those in the study area. Haddad et al. [37] provided values for c (49.9 KPa), ϕ (20.8°), γ (19.2 KN/m³), and s (0.8), while Chang et al. [38] reported data for ρ (2.1 g/cm³). These parameters, obtained through standardized laboratory tests, reflect conditions comparable to the geotechnical properties of the area under investigation.

Table 4. Soil characterization is based on laboratory analysis

Sample Code	Liquid Limit	Plastic Limit	Plasticity Index	No. 200	% Gravel	% Sand	USCS Classification
M_11	55.52	26.38	29.14	>30%	0.54	16.44	Coarse sandy clay
M_12	47.87	27.54	20.33	>30%	0.4	23.44	Sandy silt
M_13	52.41	27.78	24.63	>30%	1.15	29.56	Coarse sandy clay
M_21	56.51	29.31	27.2	>30%	4.73	7.39	Coarse sandy clay

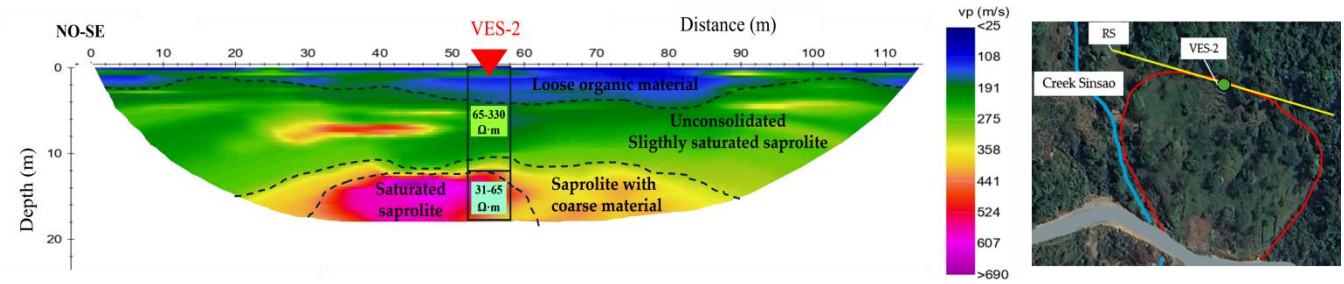

Figure 5. Tomography of RS2 (velocity) and its correlation with VES-2 (resistivity) in the N 80° W direction

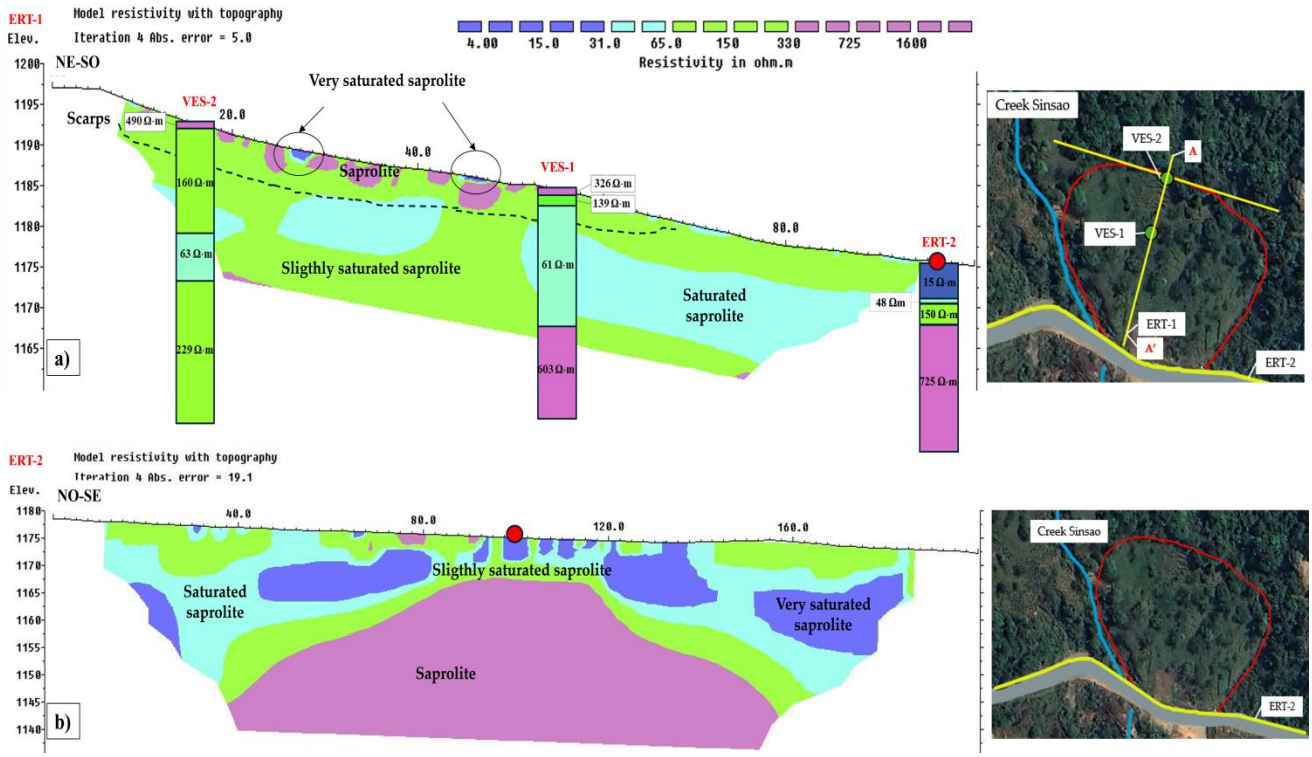

Figure 6. Geophysical correlation between ERT and VES. ERT-1 represents the A-A' profile in the N 10° E direction, and ERT-2 is in the N 80° W direction in Figure 4

3.1.2 Geophysical sections of the landslide

Seismic tomography of the upper section of the landslide (Figure 5) identifies a surface layer of very low stiffness (Vp <191 m/s), typical of loose or organic soil, over a thicker unit with velocities between 191 and 441 m/s, corresponding to slightly saturated clays.

In contrast, velocities exceeding 524m/s are observed at the base, indicating a transition to denser material with a higher water content. These materials, according to their velocity, correlate with the resistivity values described in VES-2, which consists of a surface layer with resistivity ranging from 66 to 330 Ω·m and a second layer with resistivity ranging from 31 to 65 Ω·m. In ERT-1 (Figure 6(a)), three central units were identified: a surface layer with resistivities >330 Ω·m, corresponding to loose residual material; discontinuous low-resistivity bodies (31−65 Ω·m) at depths between 3m and 5m, interpreted as saturated clay lenses; and a more consolidated, relatively dry substrate (66−330 Ω·m) that acts as the structural base of the unstable system. VES-2 reveals a four-layer subsurface sequence extending to a depth of 68 m, which is consistent with the ERT-1 units. In contrast, VES-1, located 30 m downslope beyond the scarp area, indicates a thickening of the saturated layer from 5 to 15 m, suggesting greater water retention and reduced soil cohesion. Additionally, a deeper high-resistivity layer (603 Ω·m) was identified as heavily fractured weathered rock. ERT-2 (Figure 6(b)) reveals the influence of water infiltration from the Sinsao creek, evidenced by a low-resistivity zone (31-65 Ω·m) within the first 30m, corresponding to saturated saprolite. Lenses with even lower resistivity (<30 Ω·m) and thicknesses of 5-10 m were also identified, indicating areas with high water content. Finally, a third layer with resistivity >331 Ω·m was detected, varying from 5m at the edges to a central thickness of 30 m. This layer is interpreted as denser material composed of colluvial deposits, likely the result of past mass-wasting events accumulated at the base of the slope.

3.2 Slope stability analysis

Stability analysis using the Slide2 software was performed on a profile perpendicular to the Zaruma-Sinsao highway, from the top to the base of the slope (Figure 7). The models created in Slide2 illustrate the slope behavior in two scenarios: static (Figure 7(a)) and pseudo-static (Figure 7(b))). These scenarios assume a water table at 1m depth, based on field observations, test pits, and geophysical data. The critical SF

calculated for the static scenario was 0.99. The pseudo-static analysis, incorporating seismic coefficients according to the NEC, yielded an SF of 0.55.

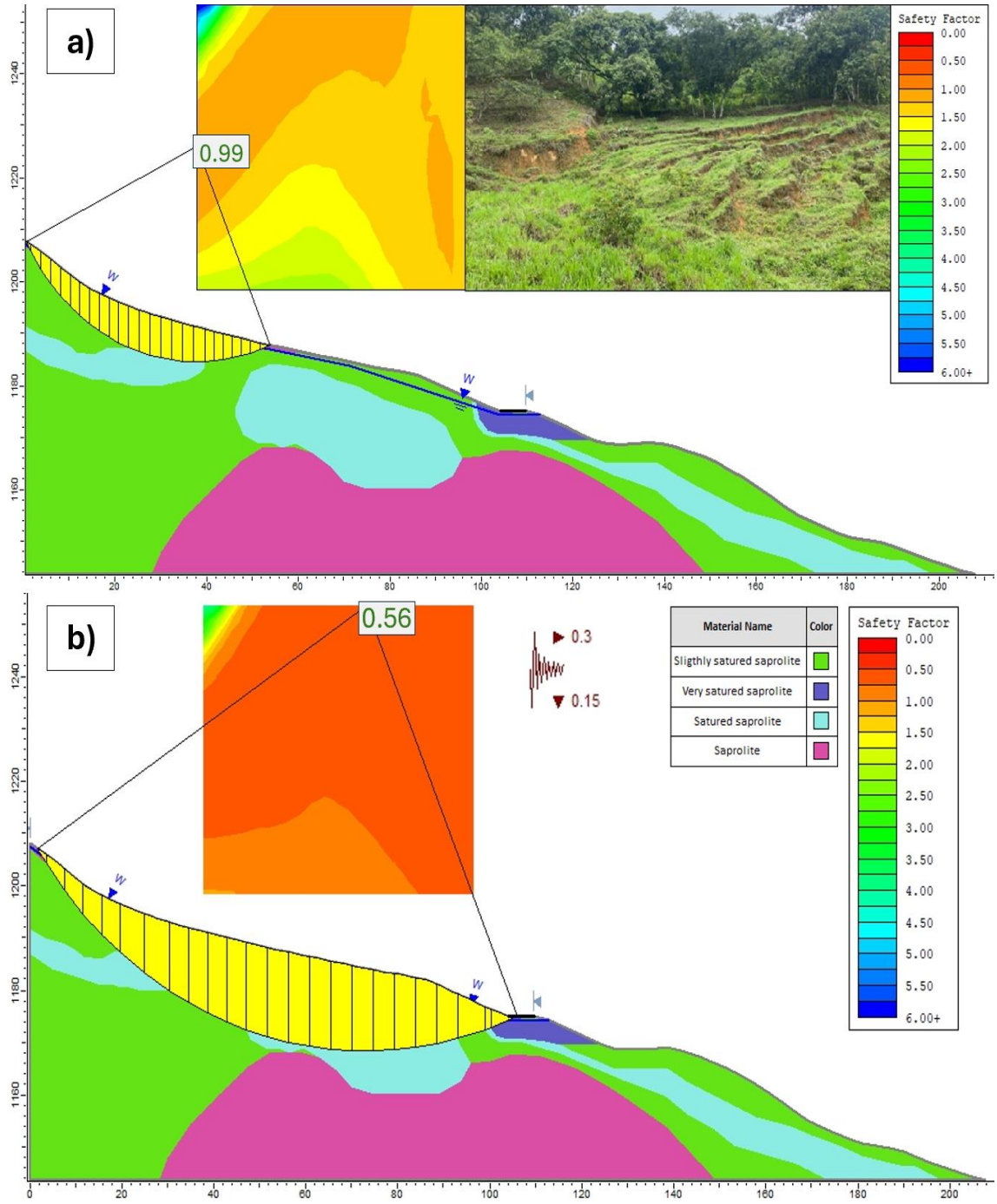

Figure 7. Slope stability A-A' profile (Figure 4) in two conditions. a) Static state with normal groundwater conditions; b) Pseudo-static model (Zh: 0.3, Zv: 0.15)

The results obtained with SAGA GIS (Figure 8) revealed a spatial distribution of stability within the landslide area. In the adopted hydrological scenario (e.g., groundwater level at the base of the soil), zones identified as potentially unstable (SF < 1.5, according to the NEC) were generated, concentrated at the toe of the slope and in the areas adjacent to the main scarps.

3.3 SWOT matrix

Based on the numerical instability observed as SF, the areas of lowest stability were identified, and the external and internal factors influencing their monitoring, study, and remediation were evaluated (Figure 9). Among the main strengths identified from the perspective of those involved, the application of software that allows for zoning and the use of non-destructive techniques as management and decision-making tools stand out. Threats affecting instability in vulnerable communities, such as the lack of funding and public policies in rural areas, and extreme events, such as rainfall, that increase saturation in unstable areas, are evident in the low FS scores according to the NEC. This analysis led to the proposal for an Early Warning System (EWS) and evacuation routes. To address resource limitations (W) and the threat of disasters (T), low-cost natural solutions

(bioengineering and artisanal drainage) and revegetation with deep-rooted species (e.g., guadua bamboo) were proposed. These measures were designed to be implemented by the neighborhood committees themselves (O), mitigating the lack of external financial support. This analysis included the identification of strengths such as the availability of geophysical data and community participation, weaknesses associated with limited accessibility to the terrain and the absence of risk response protocols, opportunities linked to the applicability of low-cost and replicable methodologies in similar areas for the creation and strengthening of academic-social links, and threats related to extreme weather events and anthropogenic processes such as deforestation or inappropriate land use.

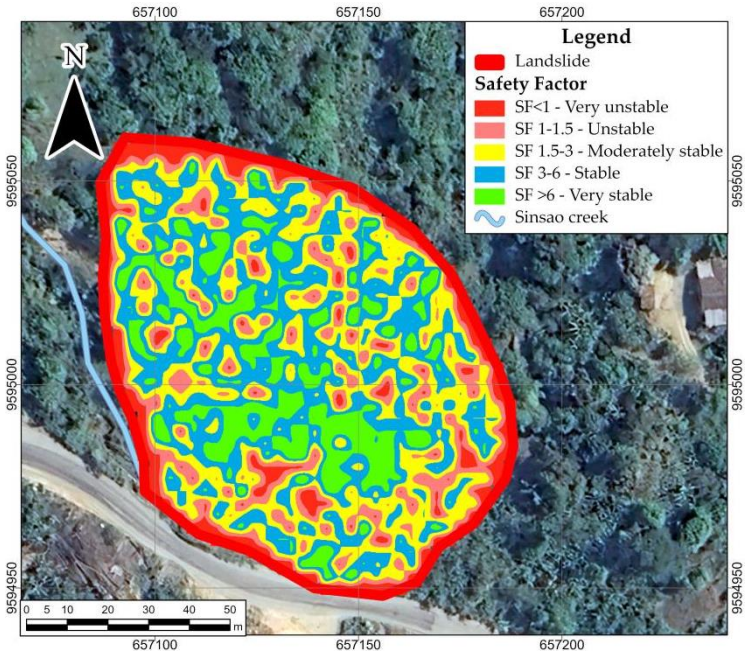

Figure 8. Map generated using SAGA GIS. Areas identified as unstable are indicated in pink and red, under the established criteria of the NEC

INTERNAL / EXTERNAL (T: Techniques, S: Social)	**Strengths (S)**	**Weaknesses (W)**
	T: Free software (SAGA GIS) adaptable to local community studies. T: Integration of non-destructive methods in roads (geophysics). S: Community organizations are present, seeking solutions. S: Visual impacts that facilitate decision-making.	T: SAGA GIS only uses the surface layer of the landslide. T: Insufficient data for analysis in Slide2 S: Lack of a community protocol for mass removal events.
Opportunities (O)	**Strategies (S+O)**	**Strategies (W+O)**
T: Application of the methodology as a territorial planning tool. T: Methodology replicable on other slopes in the area. S: Create a community guide for slope monitoring. S: Linking university-community-government in risk management. S: According to the SF, urgent intervention.	Information and training workshop for community promoters on landslides. Generate specific studies in the surrounding areas. Urgent measures for recovery and treatment at key points.	Create practical modules to address the problem using local data. Strengthen links between universities and the community for technical support.
Threats (T)	**Strategies (S+T)**	**Strategies (W+T)**
T: Lack of financial support to invest in prevention methodologies. S: More frequent extreme triggering events due to climate change and anthropogenic processes. S: Lack of public prevention/monitoring policies in rural areas.	Use of generated maps to manage an Early Warning System (EWS) and design evacuation routes or the location of remediation measures: • Promote a community-based participatory monitoring system • Implement visible signage indicating areas at potential risk of landslides To counteract the lack of financing, the landslide can be studied in phases and segmented into micro-landslides.	Design natural solutions (bioengineering and artisanal drainage) based on the results obtained and organized by neighborhood committees: • Construction of crown ditches. • Rainwater diversion through drainage channels • Protection of active escarpments with biodegradable organic mesh • Revegetation with native deep-rooted species (e.g., guadua cane, eucalyptus).

Figure 9. SWOT analysis matrix for the implementation of methodology in community settings and suggested strategies for replication

4. DISCUSSION

Geophysical correlation (ERT, VES, and RS) revealed a geomorphological and hydrogeological environment highly susceptible to mass movement processes. Saturated layers (<30 Ω·m) exhibit lateral continuity toward the base of the slope, indicating critical areas with reduced shear strength where fault surfaces may form. The unstable unconsolidated soil (<65 Ω·m) present in the study area is estimated to have a thickness of between 5 and 20 m, below which there is a body of saprolite (>331 Ω·m) at a depth greater than 20 m at the bottom of the landslide, which indicates the presence of ancient colluvial deposits, on which the road stabilization was carried out.

The model developed in Slide2 enabled simulation of the internal behavior of the slope using multilayer geotechnical profiles derived from geophysical methods (ERT, VES, and RS) and geomechanical parameters. The SF obtained under static conditions was 0.99, below the acceptable limit for the NEC, and decreased to 0.56 when seismic coefficients were applied (Zh: 0.3, Zv: 0.15) (Figure 7). This decrease is justified by the incorporation of inertial forces that amplify destabilizing forces and reduce effective friction, especially in saturated fine soils where interstitial pressures increase [39, 40].

In contrast, the stability analysis indicates that the SF values fall below the minimum threshold established by the NEC for design and construction works. The model generated in SAGA GIS shows an SF of less than 1.5 in 25.6% of the area, highlighting critical areas where the terrain may move (even without additional loads or extreme events) at the top of the slope, particularly where active escarpments and NE-oriented cracks are present These SAGA GIS results have been used to estimate possible failure zones and landslide trend lines [41]. In this sense, triggering factors (such as high rainfall and earthquakes) could trigger slope failure. Such is the case of Tamban Chimbo in the Ecuadorian Andes, which shares climatic characteristics with Sinsao parish, where moderate rainfall over 11 days triggered a large landslide [42].

However, this analysis is limited to superficial parameters, which restricts its accuracy at the local and depth scales. This method is widely used to map landslide susceptibility by calculating SF, and studies in the mountainous terrain of the Cameron Highlands, Malaysia, demonstrate its feasibility, cost-effectiveness, and time savings [43].

Compared to the methodologies applied, Slide2 allowed the identification of saturated clay units that favor deep fault surfaces. Meanwhile, SAGA GIS identified unstable areas at the surface, with the upper part of the slope most unstable, which correlates with the presence of active escarpments and saturated clay evident in the Slide2 profile. However, when comparing both results under pseudo-static conditions, SF values of 0.56 and 0.3 were obtained in Slide2 (Figure 10(a)) and SAGA GIS (Figure 10(b)), respectively.

This difference suggests that SAGA GIS tends to generate more conservative scenarios, reflecting its simplified approach based on the infinite-slope model and generalized surface parameters [29]. Unlike Slide2, which estimates the critical surface using limit equilibrium methods [32]. Although this represents a technical limitation, it can also be beneficial in preventive contexts, as it enables preliminary zoning that is more susceptible to critical surface conditions (Figure 11). This refers to the case in Portofino (Italy), a mountainous region where these maps are used to predict future landslide occurrence reliably [44]. Additionally, stability modeling using Slide2 is significantly improved when geotechnical subsoil variability and its interaction with the hydrological and seismic regimes are incorporated [45].

The integration of geomechanical parameters derived from primary studies of similar soils is well-founded, as it feeds into the stability model in Slide2 and SAGA GIS. This offers the possibility of using this type of data in the preliminary analysis of slope stability [46]. At the same time, free databases containing spatial geological information were analyzed, enabling characterization of surface soil types using GIS [47]. This secondary characterization coincided with the laboratory results, which identified coarse sandy clay as the predominant material.

This research offers a methodological framework that can be replicated in Andean areas with logistical limitations. The integration of an exploration raster model and a deterministic limit-equilibrium model provides a diagnostic that strikes a balance between operational efficiency and technical depth. The combined application of these tools enables local capacities to be aligned with realistic, context-specific mitigation strategies based on a SWOT analysis, focusing not only on reducing risk but also on optimizing resource use for geotechnical studies in hard-to-reach areas.

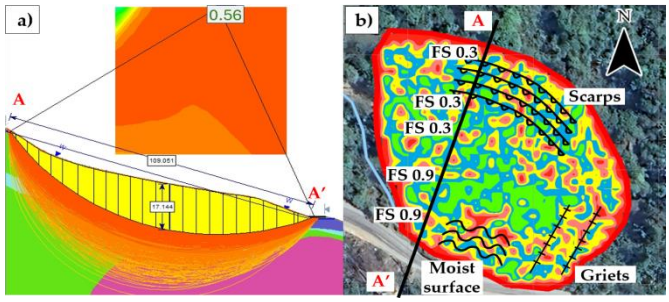

Figure 10. Comparison of SF. a) Surfaces analyzed by Slide2 and measurements of the sliding area, b) SF along the profile and in affected areas

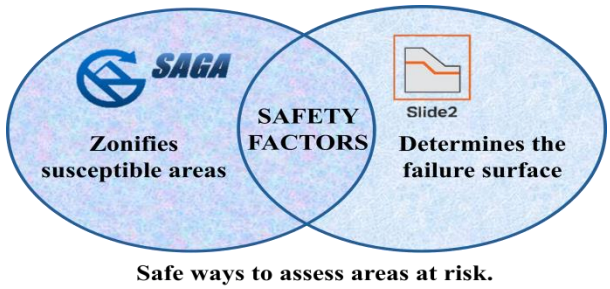

Figure 11. Integration of assessment tools for landslide-prone areas

Strategies such as revegetation have been proven effective in studies in Colombia, where increased root cohesion and decreased saturation [48] have been observed. Additionally, revegetation is the most economical and easy-to-manage method for reducing landslides in Italy [49]. These actions should be complemented by continuous monitoring of ground behavior, especially in areas where escarpment dynamics indicate active movement. Community involvement is essential for early detection of instability signs and for implementing conservation measures suited to local conditions. Protecting escarpments with natural or mixed

structures is also a key strategy to reduce landslide recurrence, highlighting the need to integrate bioengineering solutions, participatory monitoring, and sustainable land management to ensure long-term slope stability.

The study was conducted under budgetary and logistical constraints inherent to an Andean context with scarce data and limited funding for technical studies. This justified the pragmatic approach of relying on a localized field characterization (two test pits and five geophysical points) and adopting geotechnical parameters derived from literature. This dependence on indirect data introduces uncertainty, primarily in two areas: the spatial extrapolation of parameters, where the limited sampling makes it difficult to map the actual variability of soil strength properties (cohesion and friction), affecting the model inputs; and the non-singularity of geophysical inversion, where the interpretation of resistivity profiles to define the stratigraphy of the Slide2 model could vary, impacting the geometry of the critical failure surface.

The direct consequence of these limitations is that the final SF values must be interpreted as a probabilistic range rather than exact deterministic values. This necessitates caution in concluding that the sector's risk and instability are high, as the results are sensitive to unsampled geometric and parametric variations. To mitigate this limitation, it is recommended to conduct further sensitivity analyses and increase the density of in-situ characterization and specific laboratory tests such as direct shear and permeability testing.

As a future projection, a more comprehensive review of scientific articles should be conducted to extract and generate a database as a tool to complement stability studies that lack access to laboratory tests. Develop a landslide susceptibility map for the entire Sinsao parish using SAGA GIS, integrating variables such as vegetation cover, drainage, and rainfall records to improve the tool's ability to detect landslides-prone areas. This zoning would enable the identification of critical areas for prioritizing geotechnical and stability studies using Slide2 and, consequently, defining priority intervention zones. Additionally, it is recommended to assess the impact of mining vibrations on slope stability, as this is a primary economic activity in the area [20, 50-52]. This information represents technical input for decision-makers, enabling them to develop a community EWS based on participatory monitoring, low-cost weather stations, and local communication networks, strengthening resilience to geodynamic threats in an area historically exposed to mass movement events.

5. CONCLUSIONS

The applied methodology enabled a characterization of the active small-scale landslide located in the Sinsao parish. Through bibliographic, geotechnical, and geophysical analysis, coarse sandy clay was identified as the predominant material, with a critical saturated layer between 5 and 15 m thick, characterized by resistivity values below 30 Ω·m, indicating high humidity and low shear strength, which was determined to be the central fault zone. The slope stability analysis in SAGA GIS software indicated that approximately 25% of the analyzed area has an SF below 1.5, indicating unstable conditions. The Slide2 software enabled more accurate modeling of the slope's profile behavior, yielding an SF of 0.99 under static conditions and 0.56 under pseudo-static conditions, both of which are below the stability threshold defined by the NEC.

The combination of spatial analysis models in SAGA GIS with deterministic modeling in Slide2 enables a more robust assessment of slope stability in active geodynamic contexts, such as the Sinsao parish. While SAGA GIS is effective for zoning critical areas using surface-layer parameters (c, ϕ, ρ, s) and fault-plane thickness, its accuracy depends directly on the quality of the input data. Slide2 allowed the internal behavior of the slope to be modeled by incorporating geophysical profiles, geomechanical data (c, ϕ, γ), and seismic simulations, providing a more detailed analysis of the fault plane. This methodological duality not only increases diagnostic accuracy but also optimizes technical resources by prioritizing intervention areas early in the analysis.

In countries where infrastructure for slope stabilization is limited due to budgetary constraints, these integrated approaches provide diagnostics and assessments of the area, indicating priority areas for attention or assessing the mobility of people affected by this instability. The findings not only enhance technical and scientific knowledge but also generate practical tools for risk management and land-use planning, especially in rural communities. The adoption of low-cost, sustainable, and community-based measures, such as surface drainage, revegetation, and bioengineering, can serve as effective alternatives to reduce vulnerability to mass movements without relying solely on expensive structural interventions.

ACKNOWLEDGMENT

This work is supported by ESPOL Polytechnic University research project "Registry of geological interest sites of Ecuador for sustainable development strategies" with institutional code CIPAT-004-2024.

REFERENCES

[1] Zinck, J.A., López, J., Metternicht, G.I., Shrestha, D.P., Vázquez-Selem, L. (2001). Mapping and modelling mass movements and gullies in mountainous areas using remote sensing and GIS techniques. International Journal of Applied Earth Observation and Geoinformation, 3(1): 43-53. https://doi.org/10.1016/S0303-2434(01)85020-0

[2] Varnes, D.J. (1978). Slope movement types and processes. Special Report, 176(11): e33.

[3] Tofani, V., Bicocchi, G., Rossi, G., Segoni, S., D'Ambrosio, M., Casagli, N., Catani, F. (2017). Soil characterization for shallow landslides modeling: A case study in the Northern Apennines (Central Italy). Landslides, 14(2): 755-770. https://doi.org/10.1007/s10346-017-0809-8

[4] Superczyńska, M., Maślakowski, M., Mieszkowski, R. (2024). Three-dimensional interpretation of geophysical and geotechnical investigation of landslides. Archives of Civil Engineering, 70(4): 99-111. https://doi.org/10.24425/ACE.2024.151882

[5] Pereira, P.G.D.S., Coutinho, R.Q., de Souza Neto, D.P., Gomes, I.F. (2025). Stability analysis of an urban slope under human activities and critical rainfall: Case study of Recife, Brazil. Geotechnical and Geological Engineering, 43(2): 68. https://doi.org/10.1007/s10706-024-03011-z

[6] Innocenti, A., Rosi, A., Tofani, V., Pazzi, V., Gargini, E., Masi, E.B., Segoni, S., Bertolo, D., Paganone, M.,

Casagli, N. (2023). Geophysical surveys for geotechnical model reconstruction and slope stability modelling. Remote Sensing, 15(8): 2159. https://doi.org/10.3390/RS15082159

[7] Jhinkwan, V.S., Chore, H.S., Kumar, A. (2024). Assessment of stability of slopes and remedial measures in Lesser Himalayan Region: An overview. Indian Geotechnical Journal, 55(3): 2050-2072. https://doi.org/10.1007/s40098-024-01047-9

[8] Solanki, A., Gupta, V., Bhakuni, S.S., Ram, P., Joshi, M. (2019). Geological and geotechnical characterisation of the Khotila landslide in the Dharchula region, NE Kumaun Himalaya. Journal of Earth System Science, 128(4): 86. https://doi.org/10.1007/s12040-019-1106-9

[9] Bortolozo, C.A., Motta, M.F.B., Andrade, M.R.M., de Lavalle, L.V.A., Mendes, R.M., Simões, S.J.C., Mendes, T.S.G., Pampuch, L.A. (2019). Combined analysis of electrical and electromagnetic methods with geotechnical soundings and soil characterization as applied to a landslide study in Campos do Jordão City, Brazil. Journal of Applied Geophysics, 161: 1-14. https://doi.org/10.1016/J.JAPPGEO.2018.11.017

[10] Instituto Geográfico Militar (IGM). (2018). Atlas: Espacios geográficos expuestos a amenazas naturales y antrópicas, p. 108. https://www.geoportaligm.gob.ec/portal/index.php/atlas-amenazas-antropicas/.

[11] Schuster, R.L., Highland, L.M. (2001). Socioeconomic and environmental impacts of landslides in the Western Hemisphere. U.S. Geological Survey, August, 47. https://doi.org/10.3133/ofr01276

[12] Macías, L., Quiñonez-Macías, M., Toulkeridis, T., Pastor, J.L. (2024). Characterization and geophysical evaluation of the recent 2023 Alausí landslide in the northern Andes of Ecuador. Landslides, 21(3): 529-540. https://doi.org/10.1007/s10346-023-02185-6

[13] Gaillard, J.C. (2007). Resilience of traditional societies in facing natural hazards. Disaster Prevention and Management: An International Journal, 16(4): 522-544. https://doi.org/10.1108/09653560710817011

[14] Instituto de Investigación Geológico y Energético (IIGE). (2022). Geotechnical zoning project for the city of Zaruma-Portovelo. http://esacc.corteconstitucional.gob.ec/storage/api/v1/10_DWL_FL/e2NhcnBldGE6J2VzY3JpdG8nLCB1dWlkOicwY2ZhYWEwZi1kN2YwLTRlN2UtOTQ2Yy00YzRjMGVjNTFkZTIucGRmJ30=.

[15] GADP Sinsao. (2023). Development plan 2023-2027. https://gadsinsao.gob.ec/plan-de-desarrollo-2023-2027/.

[16] Instituto Nacional de Estadística y Censos (INEC). (2024). Censo Ecuador. https://www.censoecuador.gob.ec/.

[17] Reliefweb. (2015). SGR toured Sinsao parish to inspect affected areas. https://reliefweb.int/report/ecuador/sgr-recorri-parroquia-sinsao-para-inspecci-n-de-zonas-afectadas.

[18] Vikentyev, I., Banda, R., Tsepin, A., Prokofiev, V., Vikentyeva, O. (2005). Mineralogy and formation conditions of Portovelo-Zaruma gold-sulphide vein deposit, Ecuador. Geoquímica, Mineralogía Y Petrología, 43: 148-154. https://www.researchgate.net/publication/237828662_Mineralogy_and_Formation_Conditions_of_Portovelo-Zaruma_Gold-Sulphide_Vein_Deposit_Ecuador.

[19] Schütte, P. (2010). Geochronology, geochemistry, and isotopic composition (Sr, Nd, Pb) of tertiary porphyry systems in Ecuador. Section des Sciences de la Terre-Université de Genève. https://doi.org/10.13097/archive-ouverte/unige:6367

[20] Carrión-Mero, P., Solórzano, J., Chávez, M.Á., Blanco, R., Morante-Carballo, F., Aguilar, M., Briones-Bitar, J. (2020). Evaluation of geomechanical features and stability for the recommendations and rehabilitation of the Humberto Molina Hospital, Zaruma, El Oro, Ecuador. WIT Transactions on Ecology and the Environment, 241: 455-466. https://doi.org/10.2495/SDP200371

[21] ASTM International. (2017b). Test methods for particle-size distribution (Gradation) of soils using sieve analysis. Advancing Standards Transforming Markets, p. 34. https://doi.org/10.1520/D6913_D6913M-17

[22] Casagrande, A. (1948). Classification and identification of soils. Transactions of the American Society of Civil Engineers, 113(1): 901-930. https://doi.org/10.1061/TACEAT.0006109

[23] Zhdanov, M.S., Zhdanov, M.S., Keller, G.V. (1994). The Geoelectrical Methods in Geophysical Exploration. Elsevier. https://books.google.com.ec/books?id=02wZAQAAIAAJ.

[24] Schlumberger, C. (1920). Study of Underground Electrical Prospecting. https://archive.org/details/studyofundergrou00schlrich/studyofundergrou00schlrich/page/n7/mode/2up.

[25] ASTM International. (2018). Guide for using the seismic refraction method for subsurface investigation, p. 14. https://doi.org/10.1520/D5777-18

[26] Shahandashti, M., Hossain, S., Zamanian, M., Akhtar, M.A. (2021). Advanced geophysical tools for geotechnical analysis. Final Report. https://doi.org/10.13140/RG.2.2.34246.89929

[27] Martinez Vargas, A. (1990). Geotecnia Para Ingenieros: Principios Básicos. Consejo Nacional de Ciencia y Tecnología. https://books.google.com.ec/books?id=ZyTwtgAACAAJ.

[28] Reynolds, J.M. (2011). An Introduction to Applied and Environmental Geophysics. John Wiley & Sons. https://www.wiley.com/en-us/An+Introduction+to+Applied+and+Environmental+Geophysics%2C+2nd+Edition-p-9780471485353.

[29] Selby, M.J. (1993). Hillslope Materials and Processes. Oxford University Press. https://archive.org/details/hillslopemateria0000selb_a3z4.

[30] Razdolsky, A.G. (2009). Slope stability analysis based on the direct comparison of driving forces and resisting forces. International Journal for Numerical and Analytical Methods in Geomechanics, 33(8): 1123-1134. https://doi.org/10.1002/nag.761

[31] Ministerio de Desarrollo Urbano y Vivienda (MIDUVI). (2014). Geotécnia y cimentaciones. Código NEC-SE-GC. https://studylib.es/doc/9262959/nec-se-gc-geot%C3%A9cnia-y-cimentaciones.

[32] Salmasi, F., Pradhan, B., Nourani, B. (2019). Prediction of the sliding type and critical factor of safety in homogeneous finite slopes. Applied Water Science, 9(7): 158. https://doi.org/10.1007/S13201-019-1038-1

[33] Ministerio de Desarrollo Urbano y Vivienda (MIDUVI).

(2015). Peligro sísmico, diseño sismo resistente. Código NEC-SE-DS. In Miduvi. https://cicp-ec.com/documentos/NEC_2015/NEC_SE_DS_Peligro_Sismico.pdf.
[34] Bishop, A.W., Morgenstern, N. (1960). Stability coefficients for earth slopes. Geotechnique, 10(4): 129-153. https://doi.org/10.1680/geot.1960.10.4.129
[35] Duncan, J.M., Wright, S.G. (1980). The accuracy of equilibrium methods of slope stability analysis. Engineering Geology, 16(1-2): 5-17. https://doi.org/10.1016/0013-7952(80)90003-4
[36] Niemsakul, J., Hiranmahapol, S., Janmontree, J., Zadek, H., Ransikarbum, K. (2025). Analysis of barriers for hydrogen-fueled logistics under integrated sustainability: A dematel-tows framework. Journal of Cleaner Production, 513: 145720. https://doi.org/10.1016/J.JCLEPRO.2025.145720
[37] Haddad, S., Melbouci, B., Szymkiewicz, F., Duc, M., Amiri, O. (2023). Alteration under wet/dry cycles of a carbonated clay-rich soil from Azazga landslide site. Geotechnical and Geological Engineering, 41(2): 1453-1472. https://doi.org/10.1007/S10706-022-02347-8
[38] Chang, J., Xu, Y.F., Xiao, J., Wang, L., Jiang, J.Q., Guo, J.X. (2023). Influence of acid rain climate environment on deterioration of shear strength parameters of natural residual expansive soil. Transportation Geotechnics, 42: 101017. https://doi.org/10.1016/J.TRGEO.2023.101017
[39] Gong, W., Quan, C., Li, X., Wang, L., Zhao, C. (2022). Statistical analysis on the relationship between shear strength and water saturation of cohesive soils. Bulletin of Engineering Geology and The Environment, 81(8): 337. https://doi.org/10.1007/S10064-022-02811-Y
[40] Srivastava, L.S., Chakrabortty, P. (2024). Probabilistic assessment of seismic slope stability of a railway embankment. International Conference on Recent Advances in Geotechnical Earthquake Engineering and Soil Dynamics, 568: 91-99. https://doi.org/10.1007/978-981-96-1683-1_8
[41] Dinesh, S., Savitha, C., Moghal, A.A.B. (2021). Prediction of stability of an infinite slope using geospatial techniques. Stability of Slopes and Underground Excavations: Proceedings of Indian Geotechnical Conference 2020, 3: 1-9. https://doi.org/10.1007/978-981-16-5601-9_1
[42] Salinas, I., Paucar, A., Quiñónez-Macías, M., Grau, F., Barragán-Taco, M., Toulkeridis, T., Chunga, K. (2024). Geotechnical and geophysical assessment of the 2021 Tamban Chimbo landslide, northern Andes of Ecuador. Geosciences, 14(4): 104. https://doi.org/10.3390/GEOSCIENCES14040104
[43] Ming, P.L.H., Zawawi, A.A. (2021). Analysis of landslide occurrence using DTM-based weighted overlay: A case study in tropical mountainous forest of Cameron Highlands, Malaysia. Environment and Natural Resources Journal, 19(5): 358-370. https://doi.org/10.32526/ENNRJ/19/202100069
[44] Roccati, A., Paliaga, G., Luino, F., Faccini, F., Turconi, L. (2021). GIS-based landslide susceptibility mapping for land use planning and risk assessment. Land, 10(2): 162. https://doi.org/10.3390/LAND10020162
[45] Pasierb, B., Grodecki, M., Gwóźdź, R. (2019). Geophysical and geotechnical approach to a landslide stability assessment: A case study. Acta Geophysica, 67(6): 1823-1834. https://doi.org/10.1007/S11600-019-00338-7
[46] Gonzalez-Ollauri, A., Mickovski, S.B. (2021). A simple GIS-based tool for the detection of landslide-prone zones on a coastal slope in Scotland. Land, 10(7): 685. https://doi.org/10.3390/land10070685
[47] Ministerio de Agricultura y Ganadería (MAGAP). (2019). Catálogo de datos-metadatos. http://geoportal.agricultura.gob.ec/geonetwork/srv/spa/catalog.search#/metadata/0a26e971-5722-4a10-8a5e-d04298b0f017.
[48] Xu, J.S., Yang, X.L. (2018). Three-dimensional stability analysis of slope in unsaturated soils considering strength nonlinearity under water drawdown. Engineering Geology, 237: 102-115. https://doi.org/10.1016/j.enggeo.2018.02.010
[49] Galve, J.P., Cevasco, A., Brandolini, P., Soldati, M. (2015). Assessment of shallow landslide risk mitigation measures based on land use planning through probabilistic modelling. Landslides, 12(1): 101-114. https://doi.org/10.1007/S10346-014-0478-9
[50] Carrión-Mero, P., Aguilar-Aguilar, M., Morante-Carballo, F., Domínguez-Cuesta, M.J., Sánchez-Padilla, C., Sánchez-Zambrano, A., Briones-Bitar, J., Blanco-Torrens, R., Córdova-Rizo, J., Berrezueta, E. (2021). Surface and underground geomechanical characterization of an area affected by instability phenomena in Zaruma Mining Zone (Ecuador). Sustainability, 13(6): 3272. https://doi.org/10.3390/SU13063272
[51] Carrión-Mero, P., Solórzano, J., Morante-Carballo, F., Chávez, M., Montalván-Burbano, N., Briones-Bitar, J. (2022). Technical closure of the Humberto Molina Astudillo hospital and its implications for sustainability, Zaruma-Ecuador. International Journal of Sustainable Development and Planning, 17(2): 363-373. https://doi.org/10.18280/IJSDP.170202
[52] Jácome, M.C., Martinez-Graña, A.M., Valdés, V. (2020). Detection of terrain deformations using InSAR techniques in relation to results on terrain subsidence (Ciudad de Zaruma, Ecuador). Remote Sensing, 12(10): 1598. https://doi.org/10.3390/RS12101598

NOMENCLATURE

mm	millimeter
m	meters
m/s	Meter/second
m.a.s.l	meter above sea level
c	cohesion
s	saturation
KPa	Kilo Pascal
KN/m^3	Kilo Newton/cubic meter
g/cm^3	Gram/cubic centimeter
Ω·m	Ohmios meters
W	West
S	South
NE	Northeast

Greek symbols

ρ	density
γ	unit weight
ϕ	friction angle

nf nanofluid

APPENDIX

Table S1. Literature-reported studies meeting the experimental parameters

Article	Litology	c (KPa)	ϕ (°)	γ (KN/m³)	ρ (g/cm³)	DOI
Stability Analysis of an Urban Slope Under Human Activities and Critical Rainfall: Case Study of Recife, Brazil	Sandy clay	4,5	35,6			https://doi.org/10.1007/s10706-024-03011-z
Laboratory and Field Monitoring Tests of Volcanic Soil (Ta-d) Triggering Landslides in the 2018 Hokkaido Eastern Iburi Earthquake	Clay		52,6			https://doi.org/10.1186/s40677-024-00303-7
The Difference in Shear Behavior and Strength between Loess and Paleosol and Their Prediction of Unsaturated Strength	Clay	37,1	28,6		1,51	https://doi.org/10.3390/app14083301
Influence of Acid Rain Climate Environment on Deterioration of Shear Strength Parameters of Natural Residual Expansive Soil	Clay	49,9	20,8	19,2	2,1	https://doi.org/10.1016/j.trgeo.2023.101017
Experimental Studies on Some Clays Leading to Instability	Silty clay		25		2,69	https://doi.org/10.1016/j.trgeo.2023.101017
Effect of Local Cyclic Loading on Direct Shear Strength Characteristics of Shear-Zone Soil	CL				2,15	https://doi.org/10.3390/app122413024
Finite Element and Vulnerability Analyses of a Building Failure due to Landslide in Kaithakunda, Kerala, India	SM			18,55	2,48	https://doi.org/10.1155/2022/5297864
An Experimental and Numerical Study of Landslides Triggered by Agricultural Irrigation in Northwestern China	Silty clay	80	22		1,95	https://doi.org/10.1155/2020/8850381
Stability Analysis of a Weathered-Basalt Soil Slope Using the Double Strength Reduction Method	Silty clay	32,3	43,7		1,76	https://doi.org/10.1155/2020/8850381
Sustainable Slope Stability Analysis: A Critical Study on Methods	Clay	40	20	20		https://doi.org/10.3390/su14148847
Effects of Cyclic Variations of Pore Pressure on the Behaviour of a Gneiss Residual Soil	Silty sand			17,2		https://doi.org/10.1007/s10706-020-01356-9
Shear Strength and Mesoscopic Characteristics of Basalt Fiber–Reinforced Loess after Dry-Wet Cycles	Sandy clay				1,83	https://doi.org/10.1061/(ASCE)MT.1943-5533.0004225
The Formation Mechanism of Low-Angle Loess-Mudstone Seismic Landslides	Silty	11	31	18,64		https://doi.org/10.1016/j.soildyn.2024.108607